Journal of Mechanical Engineering and Sciences
ISSN (Print): 2289-4659; e-ISSN: 2231-8380
Volume 12, Issue 4, pp. 4001-4017, December 2018

DOI: https://doi.org/10.15282/jmes.12.4.2018.02.0348

Electron spins coupling of coconut shell activated nanocarbons in solid propellant on improving to the thrust stability and specific impulses

Nur Rachman Supadmana Muda[1*], I.N.G.Wardana[1], Nurkholis Hamidi[1], Lilis Yuliati[1] and Gunawan Witjaksono[2]

[1]Departement of Mechanical Engineering Brawijaya University, Malang, Indonesia.
[*] Email: Nurrudal@gmail.com
[2]Departement of Electrical and Electronic Engineering, Universiti Teknologi PETRONAS,Malaysia.
Email: gunawan.witjaksono@utp.edu.my

ABSTRACT

The role of activated coconut carbon in the combustion of solid propellant composed by ammonium perchlorate, aluminum, and hydroxyl terminated polybutadiene on improving to the thrust stability and specific impulses have been studied experimentally. Nanocarbons derived from coconut shells produces carbon compounds which dictates electron spin coupling sp^2-sp^3 when there is an increase in temperature until combustion occurs. Strong nanocarbon bonds require high temperatures and pressures to release bonds and bind oxygen. The results show that activated carbon plays a role in controlling the propellant combustion reaction and reduces thrust fluctuations. But the particle size plays a very decisive role. In micro size the activated carbon becomes a thermal load so thrust power decrease. At nano size the very wide contact area of the activated carbon accelerates the decomposition process to absorb large amounts of energy. While carbon nano as capacitors active side control the combustion reaction so that the exothermic process takes place more gradual and smoother that prolong burning time. As a result, there is an increase in heat flow that amplifies thrust stability and specific impulses.
Keywords: Nanocarbons; electron spin coupling; thrust stability; specific impulses.

INTRODUCTION

In general, solid propellant materials are more difficult to control than liquid and hybrid materials [1]. However, they are much easier to manufacture, and more effective combustion chambers only filled with propellant fuel [2]. The main disadvantage of the chemical propulsion of solid propellant is its low level of solid fuel regression leading to low rocket thrust. Several methods and techniques have been studied to address low inherent regression. Boron improves solid grain regression rate by increasing the radiative heat flux from the diffusion of the fire zone back to the fuel surface [3]. Nanoscale aluminum has the same effect, but it has a much lower ignition temperature due to its high specific surface area, resulting in the energy release being closer to the fuel surface [4]. Energetic nanoscale aluminum has been proven to be an effective catalyst in the composite solid propellant containing hydroxyl terminated polybutadiene (HTPB) and hybrid propellants with solid HTPB grains [5]. The combustion quality can be increased using HTPB on hybrid motors with the addition of nanoscale aluminum as a catalyst [6].

The properties and availability of nanoscale aluminum (nAl) have been developed in novel solid propellant formulations. The potential use of nano-size powders for rocket propulsion [7]. Some potential benefits of this element are short ignition delay, fast burning time and as energetic agent of forming material. The utilization of nAl has resulted in a significant increase in solid propellant performance [8]. The disadvantages of nAl are reduced active aluminum content, electrostatic discharge sensitivity (ESD) when dry, and poor rheological properties possibly a weakness that occurs in nanosized aluminum. Indonesia is one of the largest coconut producers in the world, until now most of the coconut can used for humans. But there is waste that is underutilized coconut products, it's coconut shell. Coconut shell has a hard layer with a thickness of about 3-5 mm consisting of lignin, cellulose, methoxyl and various mineral. Coconut shell weight about 15-19% of the overall weight of the coconut. Coconut A shell is an organic material that can produce elementscarbon by heating process. Charcoal and activated carbon is produced by heated coconut shells. Charcoal contains pure carbon produced with waste water and volatile substances [9]. The effects of temperature on the surface areas (BET and micropore) and pore volumes gradually increased with increasing final carbonization temperature until 850 °C [10]. The nanocarbon product is porous material with fractal geometry, associated with large internal surface areas and low mass densities. The Percolation transition produces porous nanocarbons with fractal geometry, which comprise most of the carbon sp^2 with pentagonal and heptagonal defects.

This work shows a simple synthetic pathways to a high surface area, low-density nanocarbons with lots of energy, and mechanical metamaterial applications, including self-improvement composite reinforcement [11]. The discussions are mainly addressed to the role of activated carbon nano specific surface area and the role of unpaired spin electron in active side of the carbon nano on the rocket specific impulse. As shown in Figure 1 unstable burning occurs when present work pressure in the motor space rises above the value of the designed motor is observed. This characterized by deep fluctuations in pressure values some parts or across the entire working range (average pressure above the assumed value), with a sudden increase in the pressure of space that can produce an explosion [12]. The structure of the composite rocket propellants is heterogeneous, and so it is wave structure of combustion. Even when the particle size AP is 10 μm (or less), it is very large compared to its size molecule [13]. The AP particles on the propellant surface are decomposes creating a gas fragment that it reacts with gas occurs by separating the polymer binder. The superiority of coconut shell nano activated carbon is to form strong carbon bonds that are not easy to remove electrons but very fast to attract other bonds, the highest melting point compared to coal and wood carbon [14]. The highest porosity compared to the carbon element in addition to the coconut shell so that it is easy to store the good heat. Active nano carbon functions as electron spin coupling when there is an increase in temperature until combustion occurs. Strong nanocarbon bonds require high temperatures and pressures to release bonds and bind oxygen. The increase in combustion temperature results in a vacancy in nano carbon, the reaction of carbon nano bonds to defend itself due to the vacancy causes nano carbon to release electrons and attract other carbon compounds to create new bonds [15]. The condition of maintaining this nano carbon bond can maintain even temperature stability on the surface of the fire zone. On the other hand, the effect of nanocarbons at the beginning of the combustion of fuel and oxidizing agents results in C-C and C-O, C-N, C-Cl bonds undergoing a greater energy absorption process [16]. Nitrogen, Cl and O elements are more directed to one vector so that more energy is produced. Significantly the role of nano carbon can affect the stability of thrust and increase specific impulses.

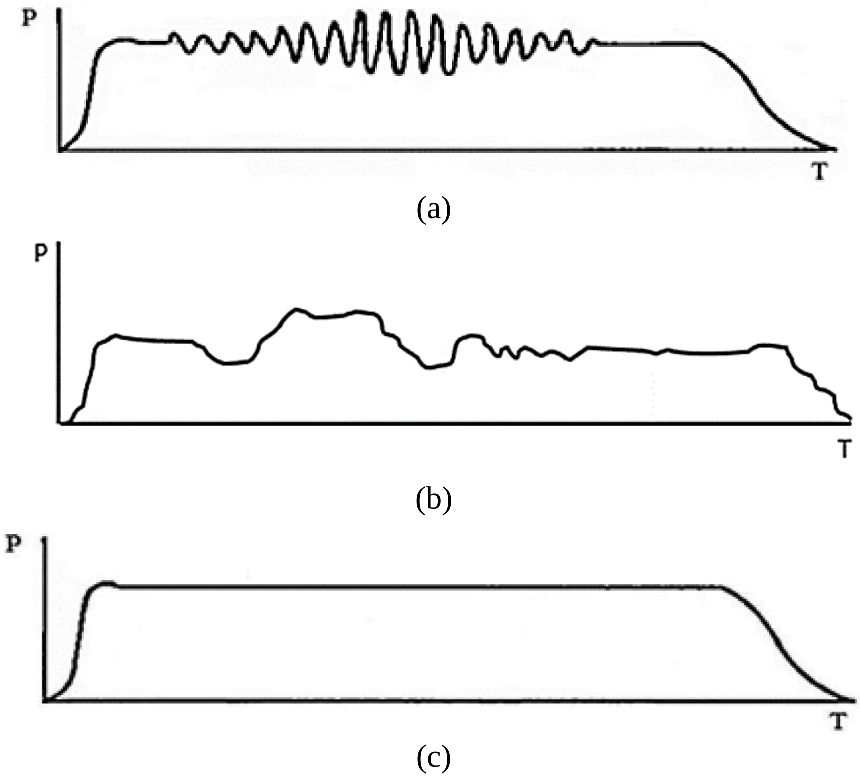

Figure 1. pressure versus time of (a) oscillatory burning, (b) irregular burning, and (c) stable burning.

In Figure 2. illustration of solid propellant composition is shown when combustion occurs in a solid propellant, the nano carbon experiences a defect and binds carbon and oxygen atoms around the nano carbon region. The released nano carbon bond can be recovered after binding the C bond chain from HTPB. This process will occur continuously until it burns completely. In this condition the process of releasing and withdrawing electrons can occur evenly throughout the carbon nano surface which can cause the spread of combustion fires to be evenly distributed and nano carbon can function as a catalyst to hold the burning time longer and produce large energy. Figure 3 shows simulations of specific impulse enhancement patterns. The graphic pattern is blue color, the specific impulse of the rocket examined by the graphical pattern is green. In the green chart pattern is expected to produce a specific impulse (*Isp*) greater. Figure 3 show the specific graph impulse pattern of blue after F1 thrust has decreased to F2 there is a decrease in temperature, pressure and force due to the lack of control function of the Al combustion process as fuel, Ammonium perchlorate as an oxidizer and HTPB as a binder so that the combustion process uneven in the fire zone experience fluctuations in temperature, gas pressure and rocket thrust. The nano carbon control function is expected to increase the value of F1 to F2 and so on as shown in Figure 3 specific impulse patterns of green graphs. The nanocarbon effect after the combustion process will continue to regulate the release and bonding of carbon in the solid propellant material regularly and quickly to recover from because the strong electron bonds in the outer bond pull the other molecular bonds, the loose and bonding process of the coconut shell of the coconut shell can increase the effect thermal so that it burns perfectly and evenly on the surface of the propellant fire zone. The length of carbon nano bonds when experiencing a vacancy requires fast time to restore bonds [16]. On F4-F5-F6-F7, the peak of thrust and persist until the nanocarbon composition has decreased the number of bonds, resulting in a decrease in temperature, pressure and thrust as shown in F8 and so on down. This condition is different from the blue line color as shown in Figure 3, where thrust immediately decreases after reaching the peak. Nanocarbon effect improves thrust oscillation so that vector F (thrust) becomes unidirectional which can increase the rocket-specific impulse.

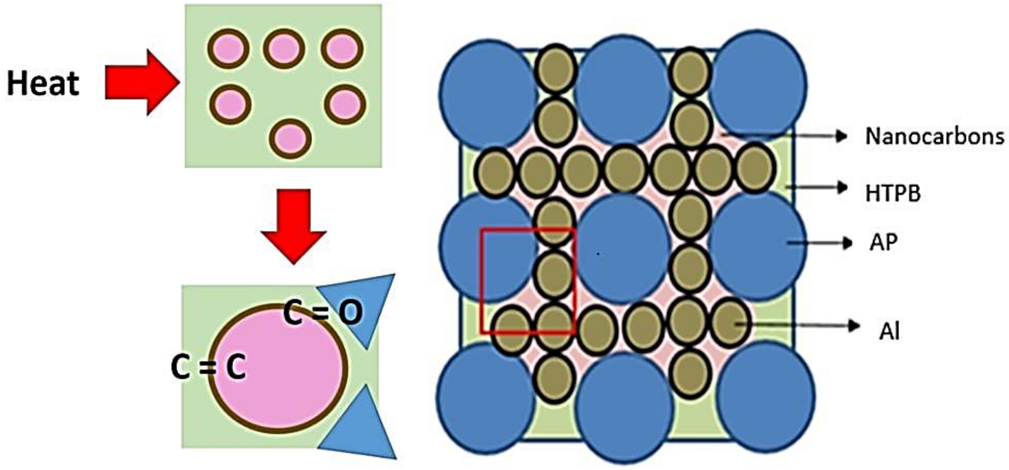

Figure 2. Illustration of solid propellant composite.

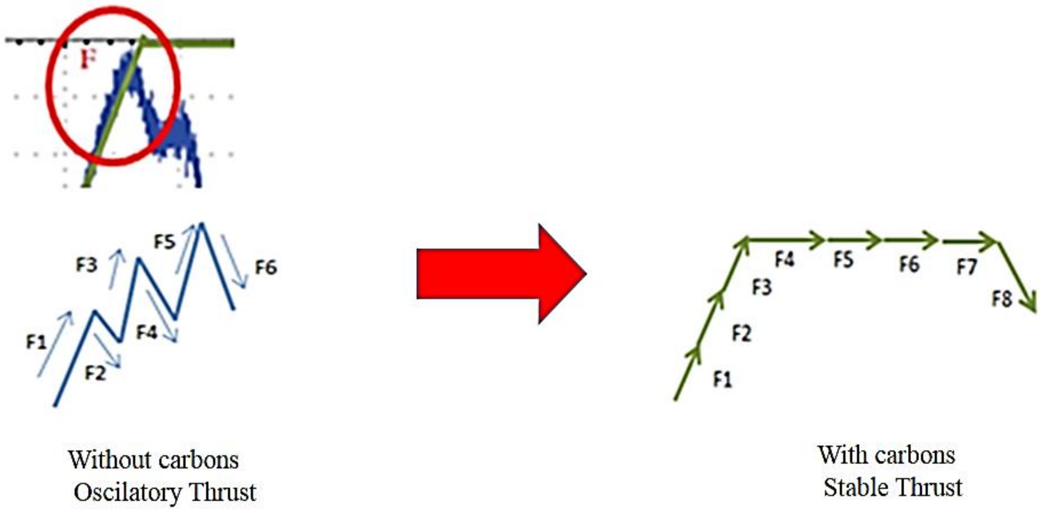

Figure 3. Simulations of specific impulse enhancement patterns.

MATERIALS AND METHODS

Elements of ACCS and NCCS

The carbon used as additive for the solid propellant was made from coconut shell. The carbon was activated and sized into two, namely coconut shell microcarbon of 200 mesh particle size (ACCS) and coconut shell nanocarbon of 100 nm particle size (NCCS). The composition of elemens in the activated carbons are listed in Table 1. When the carbon was processed into nano size the elements like Na, Mg, and Ca disappear while Si reduces. So the carbon content in NCCS increases. In this study the mass of composite solid composite test material is 200 grams. The diameter of each fuel component is *AP* 200 µm, *Al* 70 µm, activated carbon coconut shell (*ACCS*) mesh 200, nanocarbon coconut shell (*NCCS*) 100 nm, while *HTPB* is liquid binder. The composition of the fuel mixture is shown in Table 2.

Table 1 . Elements in activated carbon for ACCS and NCCS from EDX test.

Element	Wt%(ACCS)	Wt%(NCCS)
C	85.35	94.25
Na	02.35	-
Si	08.65	03.85
Ca	02.04	-
K	02.06	01.90

The stoichiometry of hydroxyl terminated polybutadiene (*HTPB*) and Ammonium perchlorate (*AP*) combustion reaction was estimated using Equation 1.

$$C_{260}H_{258}O_2 + 4{,}5NH_4ClO_4 \rightarrow 2{,}25N_2 + 64{,}5HCl + 260CO + 225{,}75H_2 - 0{,}36 \text{ kcal/gr} \quad (1)$$

The stoichiometry of *AP* and Aluminum (*Al*) combustion reactions was determined as in Equation 2.

$$2\,NH_4ClO_4 + 4\,Al \rightarrow 2\,Al_2O_3 + 2HCl + N_2 + 2H_2O + H_2 - 2{,}5 \text{ kcal/g} \quad (2)$$

Table 2. Composition of the test material.

Material	*AP* (*NH_4ClO_4*) %	*HTPB* (*$C_{260}H_{258}O_2$*) %	*Al* %	*ACCS* %	*NCCS* %	Explanation
C1	70	15	15	-	-	Stoichiometry without C
C2	70	15	10	5	-	Non stoichiometry with 5% µC
C3	70	15	10	-	5	Non stoichiometry with 5% nC
C4	70	15	15	-	5	Stoichiometry with 5% nC

Experimental apparatus

Experimental apparatus is used to determine the value of gas pressure, thrust and combustion time such as shown in Figure 5. The data acquisition for thrust and impulse specific test illustrated in Figures 4 and 5. Combustor type chamber-like geometry design has been used to get gas temperature data of fluida [15]. The propellant was burned using igniter controlled by a computer via the microcontroller. The thrust generated by propellant burning process was measured by a Load cell placed under a tube having a height of 150 mm, a diameter of 33 mm. The solid propellant having 100 mm high, 30 mm diameter was placed inside Chamber. The exhaust nozzle temperature was measured with thermocouple while the pressure in the nozzle was measured by pressure sensor. Data from load cell, temperature, and gas pressure were processed in microcontroller before sending into memory of computer. The computer shows the thrust graph of propellant combustion [14].

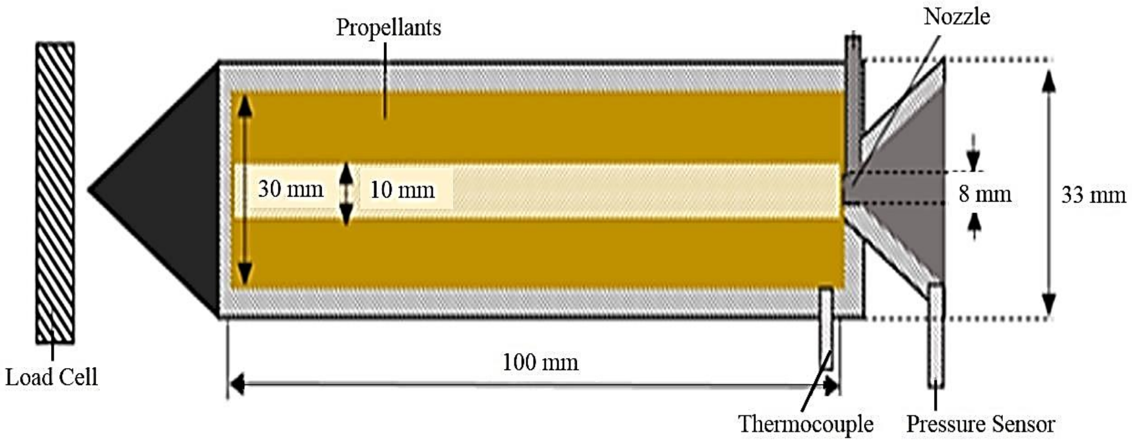

Figure 4. Chamber contains propellant materials.

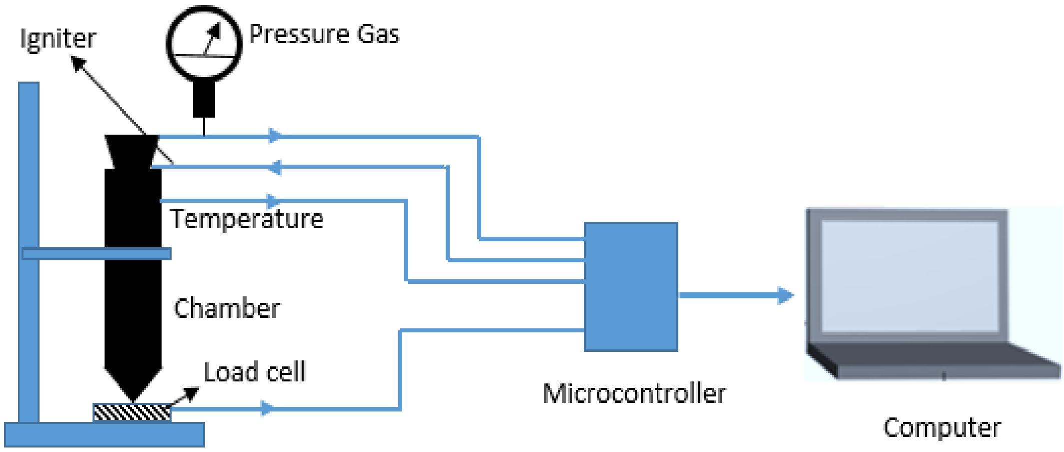

Figure 5. Experimental apparatus thrust test.

Thrust and specific impulse of rocket (Isp)

Thrust is force of rocket and the specific impulse is the force multiplied by the difference in time divided by each change in the mass of the propellant [18]. This gas pressure in the nozzle has direct effect on the thrust such as Equations (3) and (4). The specific impulse of rockets such as described in Equations (5) and (6) [18].

$$F = mdot*Ve(pe\text{-}p0)*Ae \tag{3}$$

$$mdot=r*Ve*Ae \tag{4}$$

(5)

$$F = go*Isp*\dot{m}$$

$$Isp = F/(go*\dot{m}) \tag{6}$$

Equations (3) and (4) shows that rocket thrust, F is the thrust obtained from engine, in newtons (or force), m is the mass flowrate in kg/s, m_{dot} times jet stream velocity at the nozzle exit, Ve with additional force generated by pressure different between nozzle exit pressure, pe and that in the chamber time nozzle exit area, Ae. The m_{dot} is proportional to combustion gas density, r times Ve times Ae. As shown by the result in Table 2, the addition of NCCS to the stoichiometric propellant fuel mixture produces the highest rocket thrust. Equations (5) and (6) shows g_0 is the standard gravity (9.8 m/s^2), I_{sp} (specific impulse) measured in seconds is the amount of time a rocket engine can generate thrust, given a quantity of propellants whose weight is equal to the engine has thrust. The total impulse (I) of a rocket is defined as the average thrust times the total time of firing. The total impulse such as Equation (7) [18]. Δt is the total time of propellants burns.

$$I = F* \Delta t \tag{7}$$

RESULTS AND DISCUSSION

This section presents the results from investigation, consist of comparison of the materials SEM, comparison of material atom bond spectrum, comparison of heat flow, exothermic and endothermic process, comparison of gas pressure, effect of nanocarbons on improving the thrust stability and specific impulses.

SEM of Materials

Scanning Electron Microscope (SEM) SU 5000 used to determine the morphology and porosity of the material. Figure 6 shows SEM image of composite solid propellant. Figure 6 (a) shows a mixture of AP, Al and HTPB with the composition of C1. The fuel structure looks quite dense because HTPB binds the AP and Al strong enough [14, 15]. In the composition of C2 (Figure 6 (b)) the fuel structure appears less dense than the composition of C1. This is due to the contact area of micro size of carbon is small so that the HTPB has the less homogeneous contact and binds the surface of activated carbon as shown in Figure 6 (e). Figure 6 (f) presents a very large surface of nanocarbon making it easy to bind Al and AP compared without carbon (C1) as well as using micro carbon (C2). Figure 6 (c) shows the fuel structure with the composition of C3 higher density than the compositions C1 and C2. The very wide nanocarbon surface makes it easy to bind Al and AP compared that without carbon (C1) as well as using micro carbon (C2). With the composition of C4 as in Figure 6 (d) the density of the fuel structure is strongest. This is because in the stoichiometric mixture almost all of the solid components of the propellant are bonded to the surface of the nano carbon catalyst. It appears that nanocarbon is an important factor in binding Al and AP. Table 1 shows that NCCS contains more C than ACCS while ACCS contains more Mg, Ca, Al, Na and Si. These elements need more ionization energy than C. Therefore, NCCS is more active than ACCS because NCCS contains more carbon element.

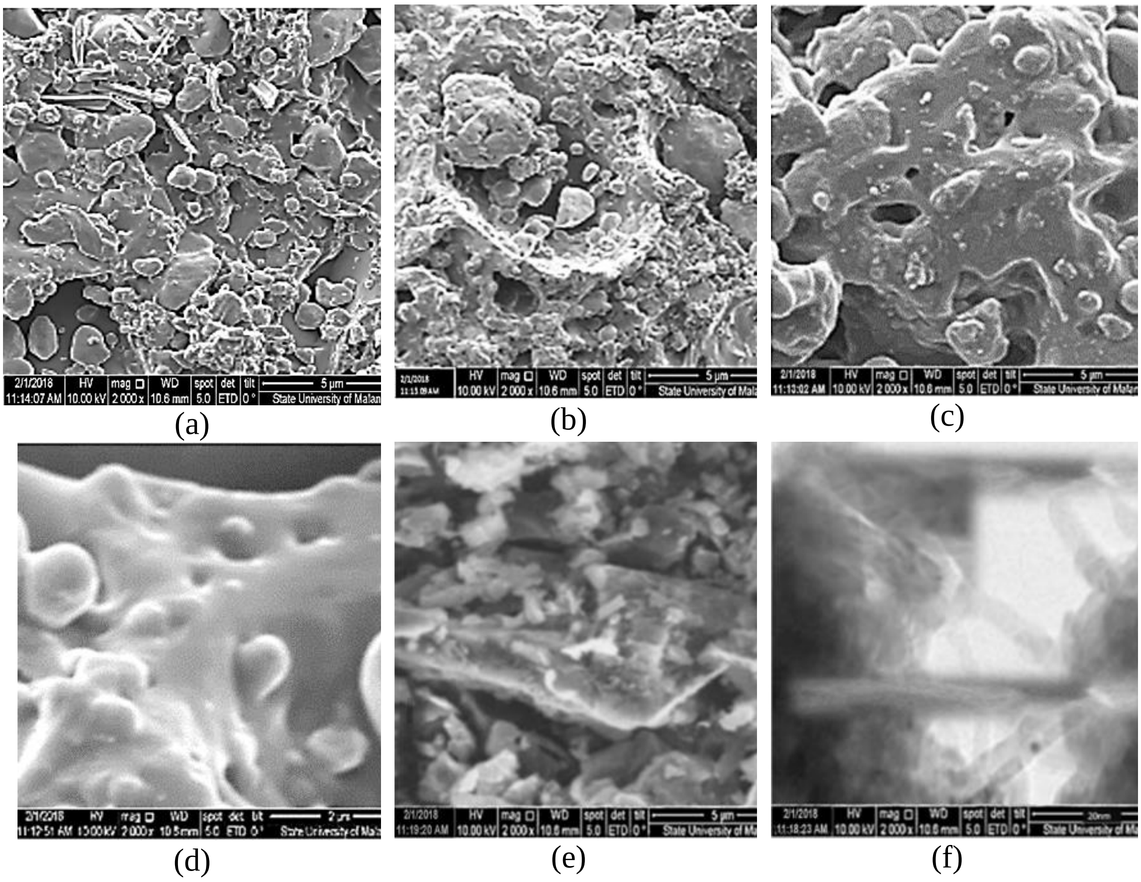

Figure 6. SEM of (a) C1, (b) C2, (c) C3, (d) C4, (e) ACCS, and (f) NCCS.

Electron spins coupling of coconut shell activated nanocarbons

Nanocarbons of coconut shell activated are similar graphene [16]. Graphene to wrap micro-sized aluminum is mixed with HTPB and AP is given a thermal effect and is seen using ESCA [18]. As shown Figure 7, spectrum of atom bond in the sample was revealed using an ESCA measuring instrument (electron spectroscopy chemical analysis. Figure 7 show the C1 peak is located at 282.20 eV associated with O=C–OH for sp^2 carbon. The composition of O=C–OH part in carbon is 7.32 in%. C2 peak at 281.08 eV works for sp^3 –C–O–C– based groups in shown Figure 7. The peak of C3 appears at 285.14 eV according to –C–C– of the original sp^3. The overall range of C4 peak intensity, shows that, π bond dopants also exist because the oxygen portion is adsorbed physically. Figure 7 shows C4 peak at 285.82 eV works for sp^3 –C=C– resonance based group. The π bond dopant is available in C4 in the form of a bound hole. In general, C4 contains genuine 7.75% oxygen. Using ESCA analysis shows that, C4 contains 90.11 in carbon % and 7.75 in % oxygen in the form of –C=C– resonance. Exchange interactions can be dominant in oxygen sites that exchange pair holes, on oxygen sites. So the electron spins coupling exchange can be dominant in sp^2- sp^3, because of the availability of electrons in attractive force of π bond. This shows that the total of sp^3 content is relatively high compared to sp^2. In this condition C4 appears on the most stable bond with the largest binding energy. This affects the stability of combustion which an increase the stability of thrust and rocket specific impulse.

Heat flow of solid propellant materials

Differential Scanning Calorymetry (*DSC*) Q20 is used to determine heatflow processes, exothermic andendothermic peaks [19]. Heatflow measurements show time sequence burning flame as shown in Figure 8. In the C1 composition, the flame jets are strong enough, but the flame propagation tends to be tilted resulting in wiping flame so that the gas jet stream to the axial direction (*Ve*) becomes weaker and therefore the thrust is low as explained in equations (3) and (4). The skewed and wiped flame propagation might be due to the inhomogeneous mixing conditions of Al and AP as evidenced by Figure 8. As a result, the melting point becomes un-patterned. Irregularity of direction of flame propagation causes thrust fluctuations. With the addition of ACCS micro activated carbon (composition C2) the fire burst becomes more regular and burning gas goes upright but the flame becomes thinner indicating weaker burning than the composition of C2 as shown in Figure 8. Regularity of combustion shows the action of micro activated carbon catalyst. The low combustion rate is due to 5% reduction of the amount of Al in conjunction with the small contact area of micro activated carbon so that does not optimally act as an intermediary reaction of AP and Al.

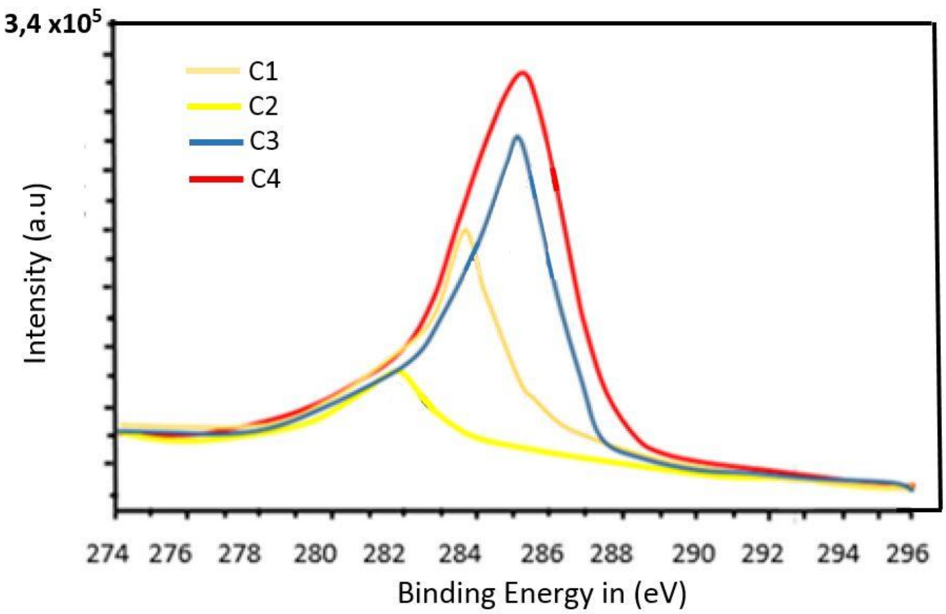

Figure 7. Comparison of material atom bond spectrum.

As a result, carbon tends to absorb heat which inhibits the decomposition process, leaving residuals as seen at the end of combustion. By replacing the micro activated carbon with nano-sized activated carbon, NCCS (C3 composition) the fire burst becomes stronger and larger than C1 and C2 as shown in the Figure 8. This occurs because at nano size (10 nm) the carbon has a much wider contact area so that the endothermic decomposition process becomes faster at lower temperatures and results in a large exothermic reaction process indicated by a sturdy flame form. As the composition of C3 was added 5% Al so that the propellant becomes stoichiometry on C4 composition then the decomposition process becomes faster while the heat release process (exothermic) becomes more controlled and lasts longer as shown in the Figure 8. This result shows that 5% nano activated carbon coconut shell acts as a capacitor to regulate energy in the reaction zone, resulting in a more patterned melting point in the reaction zone. This mechanism accelerates the decomposition or absorption of energy faster at lower temperatures and produces a large exothermic resulting in the largest form of flame. A large flame and a perpendicular pattern of flame propagation is an important factor in generating thrust to obtain a large specific impulse. Figure 8 shows the results of the DSC test for solid-propellant on various compositions of the mixture. The slope of the curve represents heat capacity. The positive slope signifies heat storage capacity or endothermic process during chemical decomposition while the negative slope signifies heat discharge capacity or the exothermic process of the combustion reaction. As shown in Figure 8 (a) a propellant combustion heat flow with C1 composition or solid composite propellant without carbon catalyst indicates the decomposition process starts at a temperature of about 271^{o}C which absorbs heat up to about 362^{o}C while the exothermic combustion reaction process takes place from 362^{o}C to 416^{o}C. At the beginning of decomposition is very slow then increases and becomes very fast at 416^{o}C. Likewise, the exothermic process very quickly at the beginning then slows down. This shows that the decomposition rate and the combustion reaction do not occur simultaneously. As a result, the thrust fluctuates, and this condition yields a heat flow of 1553 J/g. Figure 8 (b) shows that combustion of propellant with composition C2 using micro activated carbon catalyst, atomic bond more difficult to decompose, that is just starting to decompose at temperature 302^{o}C and combustion process happened at temperature of around 490^{o}C. Endothermic decomposition and exothermic reactions occur twice.

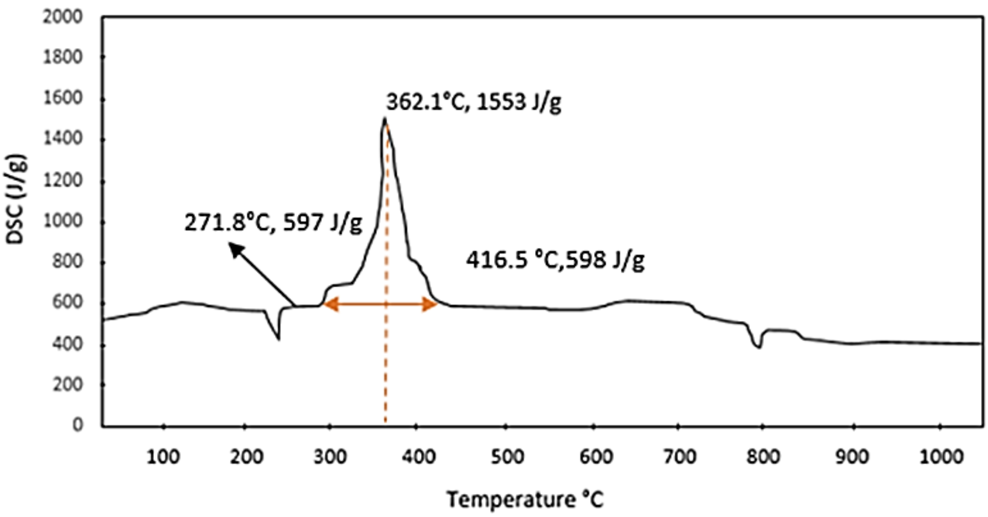

(a)

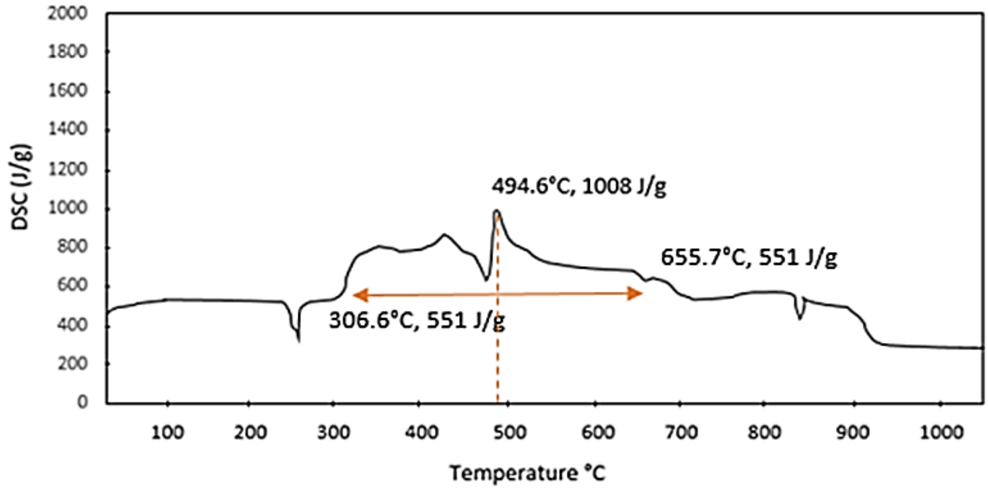

(b)

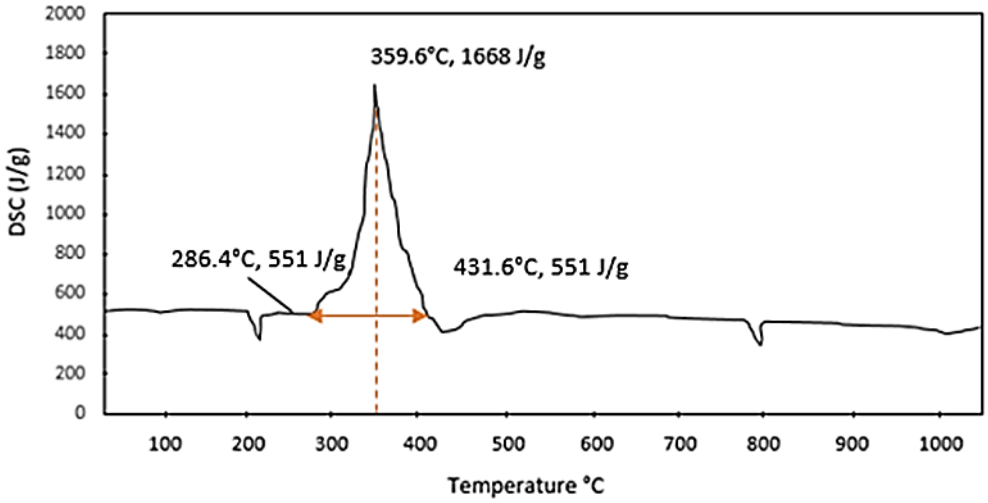

(c)

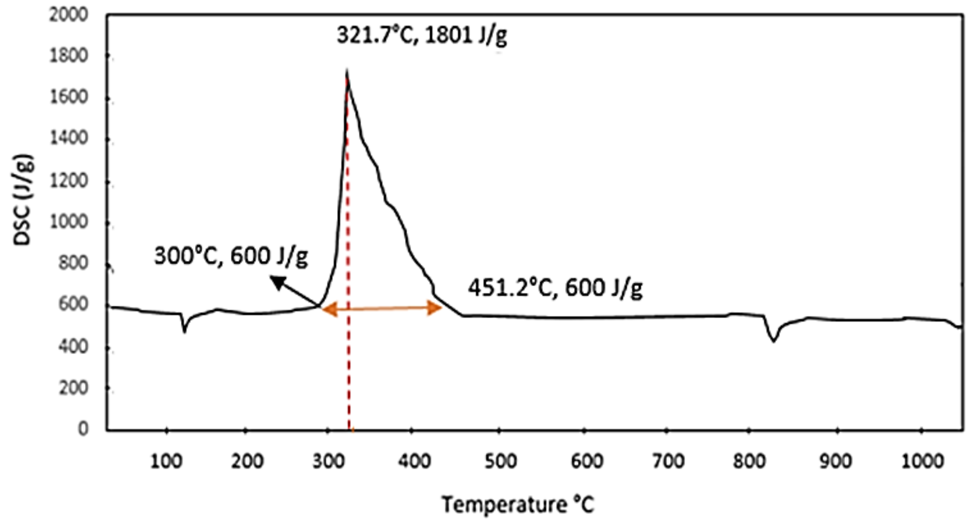

(d)

Figure 8. DSC heat flow test verses. temperature °C (a) C1, (b) C2, (c) C3, and (d) C4.

Although the heat release process proceeds to a high temperature of about 655°C but the heat flow is low, so the energy produced is lower than C1. This happens because the contacts area of activated micro carbon is small so that the reaction is difficult, and carbon tends to become a thermal load. In addition, reduction of Al by 5% becomes another cause. This condition minimizes the heat flow by only 1008 J/g. The exothermic peak occurred at 494.6°C indicating slower C2 reacts toward the exothermic peak than C1. This causes the trust to be small. Figure 8 (c) shows that as micro activated carbon in C2 is replaced by activated nanocarbon to become C3 composition the result is that nanocarbon performs its role in rapidly decomposing and improving the exothermic reaction process even if Al fuel is reduced by 5%. This happens because the contact area of carbon in the nano size is much wider than the micro carbon. Nanocarbon works more effectively making atomic bonds easily decompose and occurs in almost instantaneous time with enormous energy in the reaction zone. Heat flow increased to 1668 J/g. The endothermic peak occurring at 359.6°C indicates the carbon nano makes C3 decompose faster than C1 and C2. Figure 8(d) shows that by adding C3 with Al 5% to become stoichiometry on the composition of C4 carbon nano as capacitors triggers the endothermic decomposition process becomes much faster and occurs simultaneously and controls the gradual exothermic reaction process. As a result, the final temperature of heat release to be high that is about 451°C and heat flow for burning C4 to be very high that is equal to 1801 J/g. This condition is shown by data in Table 3. Exothermic peaks occurred at 321.7°C showing the fastest C4 reacting to exothermic peaks compared to C1, C2 and C3. As shown in Figure 8, propellant with C4 composition yields a 129.5°C exothermic process larger than C1 and C3. It is used to increase combustion time on the propellant composite, while the release energy conditions that tend to increase in the reaction zone can be used to raise the rocket thrust which also significantly increases the value of the rocket-specific impulse. The combustion process tends to be stable on the nanocarbon element, resulting in a uniform combustion pattern on the surface of the reaction zone [18]. The homogeneity of the burn gas stream direction can increase the thrust and the specific impulse of the rocket. This can happen because the contact surface of NCCS is so large that it is easy to receive heat energy to boost electron energy to escape easily. The loss of electrons in each carbon bond especially in active side result in an unpaired spin of electrons which force carbon bonds to attract other bonds quickly. As shown in Figure 8(d) the heat flow of the C4 propellant composition tends to be most stable. The stable conditions produce enormous and uniform energy because the bonds of missing electron can work together to keep themselves from the melting force in the reaction zone [19]. Hence there is no fluctuating force which can reduce the thrust value and the specific impulse.

Table 3. Comparison of exothermic peak temperature and heat flow.

Material	Exothermic Peak Temperature ° C	Endothermic Process	ΔThe Exothermic Process	Heat Flow (J/g)
C1	362.1	251.3	54.4	1553
C2	494.6	263.6	161.1	1008
C3	359.6	215.1	72	1668
C4	321.7	121.7	129.5	1801

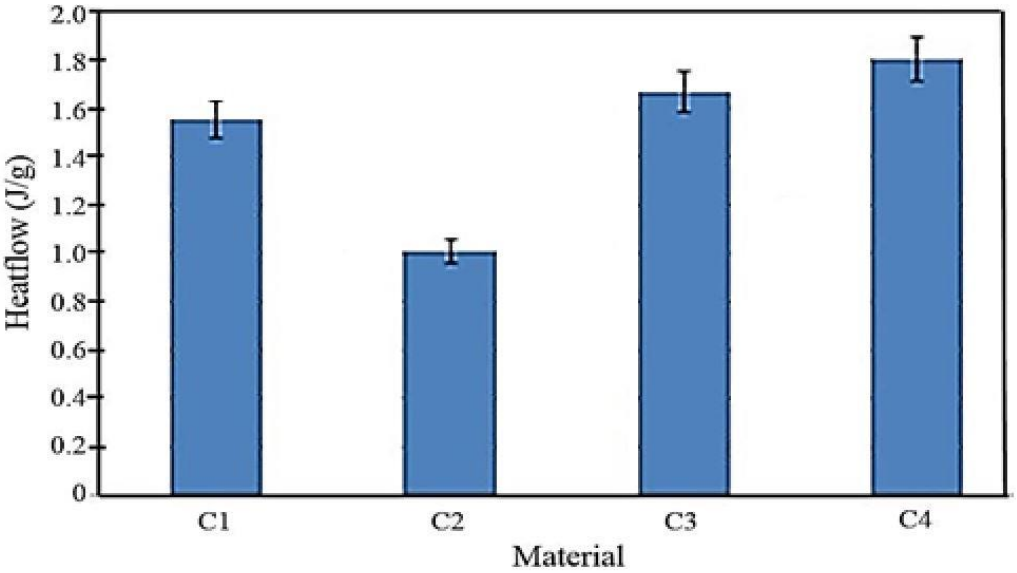

Figure 9. Comparison of materials heat flow peak.

When compared between the four test materials as presented in Figure 9 then the best order based on the reaction speed reaches the top of exothermic peak is C4. It appears that the role of activated nano carbon results in a larger heat flow which is important factor for improving thrust and specific impulses.

Thrust and Specific Impulses Results

As shown in Figure 10 the gas pressure average at the nozzle become composition C1 is P =11.5 Bar, and composition C2 show gas pressure drops to P = 8 Bar contains ACCS, eventhough the gas pressure drops but the gas pressure is more stable than C1gas pressure. However, a solid propellant containing C3 can produce P = 13 Bar, because C3 contains nanocarbons which can increase gas pressure more stable and stronger. The gas pressure is most generated by the composition of C4 can produce P = 15 Bar, because the fuel mixture is stoichiometry.

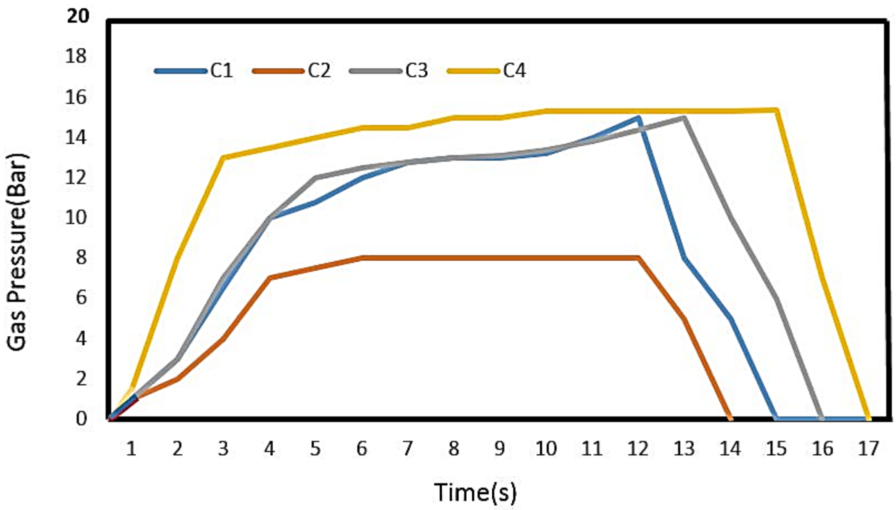

Figure 10. Gas pressure comparison of the material.

In accordance with equations [5] and [6] then conducted testing on solid propellants using instrument tool of thrust and gas pressure continues [21]. As shown in Figure 10, C1 produces gas pressure decreases, evidently effect of carbon micro lowering the value of gas pressure 3.5 Bar. However, the gas pressure average increases 5 Bar when nano carbon is used as catalyst, this occurs at the interval of C2 to C3. The stoichiometric composition using nano carbon as the catalyst made gas pressure average to increase 2 Bar at intervals C3 to C4. C4 in stoichiometric conditions that the amount of Al as fuel is added to 5% which can increase the gas pressure. Thus, using micro carbon in solid propellants can decrease gas pressure in the nozzle, but using carbon nano as a catalyst that can increase gas pressure in the nozzle [20,21]. As shown in Figure 11, curve of C2, C3, C4 are stable burning because the influence of carbon serves as a capacitor that causes aluminum particles to burn evenly and stable combustion. However curve of C1 is oscillatory burning caused C1 contains the surface of aluminum particles coated by HTPB, it burns unevenly resulting unstable combustion.

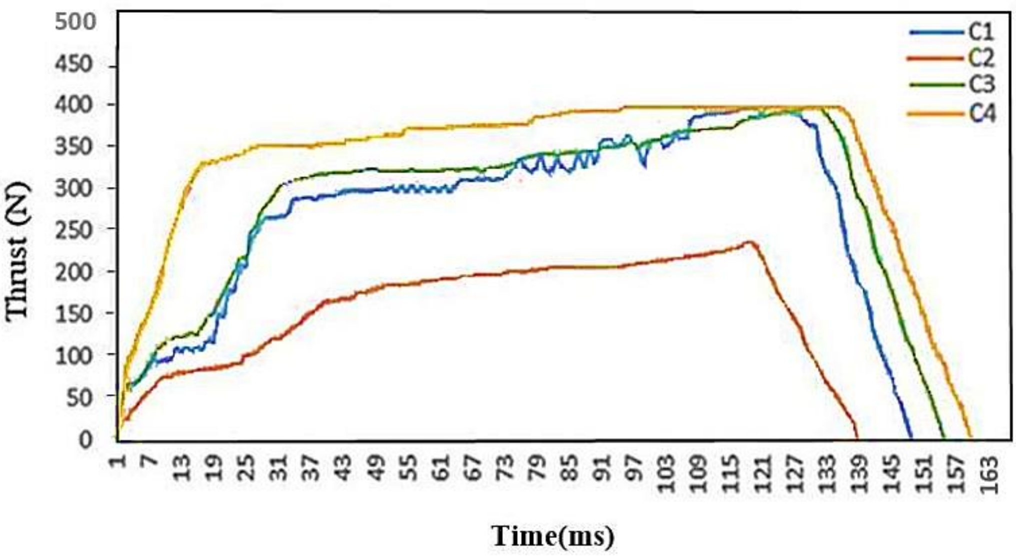

Figure 11. Comparison of the thrust of each material.

As shown in Figures 11 and 12 shows comparison peak and average thrust of C1, C2, C3 and C4. In C1 to C2 interval, thrust drop due to the influence of cabon micro as a catalyst. Thrust rises when using carbon nano as shown in C2 to C3 interval. Peak and average thrust toward the most powerful when stoichiometry of solid propellant composition using carbon nano as a catalyst occurs at C3 to C4 interval. Figure 11 shows time of thrust and specific impulse shown by the area under curve. It appears that the thrust fluctuates due to an unstable combustion process in the reaction zone.The uneven melting point of propellant in the reaction zone due to less homogen propellant results in the non-directional rocket forces vector and the uneven decomposition of atoms in the reaction zone [22]. Investigating the effect of coconut shell activated carbon as shown in Figure 12. C1 produces an average thrust: 277.57 N. However, thrust of C1 more unstable than thrust of C2 because C1 does not use coconut shell carbon as a catalyst. Figures 12 and 13 shows the comparison of thrust peak and specific impulse. C2 produce an average thrust: 159.56 N, burn time: 1.39 s, total impulse: 221.79 Ns and specific impulse (Isp): 110.9 s is lower than Isp of C1. Micro activated carbon in the composition of C2 is replaced by active nanocarbons to become a composition of C3.The results of the investigation show that the C3 thrust is more stable and greater than C1and C2. Because of the large nanocarbon contact area. As a result, Al, AP and HTPB burn together in the reaction zone in a large boost compared to C1 and C2.

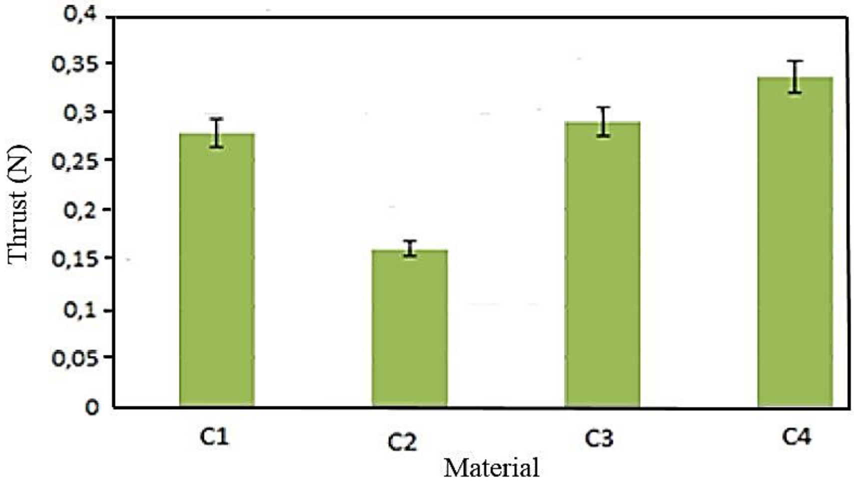

Figure 12. Comparison of thrust peak.

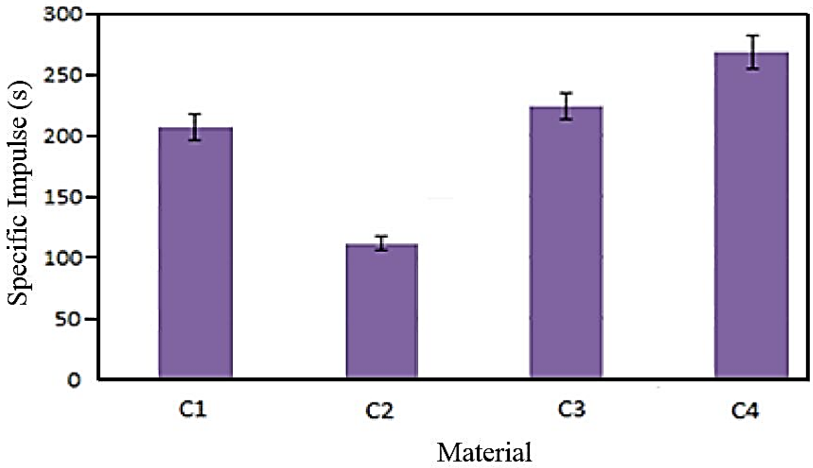

Figure 13. Comparison of specific impulse.

This condition produces an average thrust: 288.91 N, burn time: 1.55 s, total impulse: 447.81 Ns, and specific impulse (Isp): 223.91 s is higher than Isp of C1 and C2. When the composition of C3 is added 5% Al to be stoichiometric as the composition of C4 or composite solid propellant using 5% carbon nano coconut shell activated carbon is pushed to be the most stable, the largest and longest burning time. Because the heat of combustion at the stoichiometric composition is sufficient for activated carbon to regulate the combustion of aluminum, AP and HTPB. The composition of C4 produces an average thrust: 334.84 N, burning time: 1.60 s, total impulse: 535.74 Ns, and specific impulses (Isp): 267.87 s are the highest. The comparison of all materials shows that the C4 propellant material produces the strongest average thrust and the largest specific impulse peak. The effect of nanocarbon on the stoichiometric propellant mixture produces the longest combustion time, the strongest thrust and the specific impulse compared to the composition of other ingredients.

CONCLUSIONS

The addition of activated carbon into the solid propellant of Al, AP and HTPB yields the following conclusions. In general, activated carbon stabilizes rocket thrust but when activated carbon particles are in micro size, the contact surface area is so small that activated carbon tends to be a thermal load which reduces heat flow thereby weakening thrust. In nano size the activated carbon particles affect the surface morphological structure more widely than the micro carbon. Large areas and densities produce the best propellant material. Coconut shell activated nanocarbons makes the surface of the particle becomes very wide so it is easy to receive thermal energy which boost electron to escape causing unpaired electrons. The unpaired electrons in each of the strongest carbon bonds on the active side of the carbon cause the electrons to spin attracting other bonds, thus speeding up decomposition. Attractive force between atoms due to spin electrons makes nano-activated carbon act like a thermal capacitor. Nanocarbon as a capacitor accelerates decomposition at low temperatures and controls the exothermic reactions gradually resulting in higher heat flow and gas pressure and greater flame burst. The use of nanocarbons as catalysts and propellants under stoichiometric conditions makes the propellant becomes denser and increases thrust with large specific impulses. The electron spin coupling C4 exchange can be dominant in sp^2 - sp^3, because of the availability of electrons in the π bond. This condition produces the best stability and energy binding from C1, C2 and C3. This is used to increase thrust stability and impulse spesific rocket.

ACKNOWLEDGEMENTS

This research supported by Poltekad College, Malang, Indonesia and Departement of Mechanical Engineering Brawijaya University, Malang, Indonesia.

REFERENCES

[1] Thomas JC, Petersen EL, Sain JDD, Ridlehuber MN, Brady BB. Hybrid rocket burning rate enhancement by nano-scale additives in HTPB fuel grains. American Institute of Aeronautics and Astronautics; 2014.

[2] Siva V. Investigation of solid propellant rocket engine. International Journal of Engineering Research and Application. 2017;7:73-75.

[3] Liu LL, He GQ, Wang YH, Hu SQ. Chemical analysis of primary combustion products of boron-based fuel-rich propellants. RSC Advances. 2015;5: 101416-26.

[4] Minseok, Oh MC, Han DH, Jung SH, Ahn BM. Exothermic reaction kinetics in high energy density Al-Ni with nanoscale multilayers synthesized by cryomilling. Metals. 2018;8:121.

[5] Shark SC, Zaseck CR, Pourpoint TL, Son SF. Solid-fuel regression rates and flame characteristics in an opposed flow burner: Journal Of Propulsion And Power; 2014.

[6] Abdalla S, Wafi RAL, Pizzi A. Stability and combustion of metal nano-particles and their additive impact with diesel and biodiesel on engine efficiency. Journal of Renewable and Sustainable Energy 9; 2017.

[7] Young G, Wang H, Zachariah MR. Application of nano-aluminum/nitrocellulose mesoparticles in composite solid rocket propellants. Propellants Explos. Pyrotech. 2015;40: 413-18.
[8] DeLuca LT. Overview of Al-based nanoenergetic ingredients for solid rocket propulsion. Defence Technology; 2018.
[9] Erlinda S, Boi TD, Futri W, Esmar B. Coconut shell activated carbon as an alternative renewable energy. Indonesia EBTKE-ConEx; 2014.
[10] Ma HT, Ho VTT, Pham NB, Nguyen DC, Vo KTD, Ly HC, Phan TD. Effect of the carbonization and activation processes on the adsorption capacity of rice husk activated carbon. Vietnam Journal of Science and Technology. 2017;10: 494-502.
[11] Nomura K, Kalia RK, Li Y, Nakano A, Rajak P, Sheng C, Shimamura K, Shimojo F, Vashishta P. Nanocarbon synthesis by high temperature oxidation of nanoparticles. Nature; 2016.
[12] Chaturvedi S, Dave PN. AP/ HTPB composite propellants. Arabian Journal of Chemistry: King Saud University; 2015.
[13] Rodic V, Fidanovski B. Burning stability of composite solid propellants Including Zirconium Carbide. Scientific Technical Review. 2013;63:33-40
[14] Muda NRS, Wardana ING, Hamidi N, Yuliati L, Budi A. The total impulse study of solid propellants combustion containing activated carbon from coconut shell as a catalyst. Merdeka University of Malang Indonesia; 2017.
[15] Treedet W, Suntivarakorn S. Effect of various inlet geometries on swirling flow in can combustor. Journal of Mechanical Engineering and Sciences. 2018;12: 3712-23.
[16] Wachid FM, Perkasa AY, Prasetya FA, Rosyidah N, Darminto. Synthesis and characterization of nanocrystalline graphite from coconut shell with heating process. American Institute Physics Conference Proceedings; 2014.
[17] Astarlioglu E. Simulation of carbon nanostructures with a vacancy present. Metropolia University of Applied Sciences; 2018.
[18] Fahd A, Mostafa HE, Elbasuney S. Certain ballistic performance and thermal properties evaluation for extruded modifed double base propellants. Cent. Eur. J. Energ. Mater. 2017;14: 621-635.
[19] Sui H, Li B, Wen JZ. Interaction between single walled carbon nanotubes and reactive nanoparticle constituents in multilayered Al/NiO nanocomposite. Applied Energy Materials; 2018.
[20] Math MC, Manjunath MS. Development and characterization of cerium oxide catalyst supported on ceramic honeycomb substrate to reduce emissions of spark ignition engine. Journal of Mechanical Engineering and Sciences. 2016;10: 1956-67.
[21] Cook R, Nabity JA, Daily JW. Characterizing propellants for variable-thrust/ specific impulse colloid thrusters. Journal of Propulsion and Power. 2017; 6: 1325-31.
[22] Hasan M M, Rahman M M. Homogeneous charge compression ignition combustion. Advantages over compression ignition combustion, challenges and solutions. Renewable and Sustainable Energy Reviews. 2016;57:282-91.